SOLVING AN INVERSE KINEMATICS PROBLEM FOR A HUMANOID ROBOT'S IMITATION OF HUMAN MOTIONS USING OPTIMIZATION

ChangHwan Kim, Doik Kim and Yonghwan Oh
Intelligent Robotics Research Center
Korea Institute of Science and Technology
P.O. Box 131, Cheongryang, Seoul 130-650, Korea

Keywords: Human Motion Imitation, Inverse Kinematics Problem, Motion Capture System, Optimization.

Abstract: Interactions of a humanoid with a human are important, when the humanoid is requested to provide people with human-friendly services in unknown or uncertain environment. Such interactions may require more complicated and human-like behaviors from the humanoid. In this work the arm motion of a human is discussed as the early stage of human motion imitation by a humanoid. A motion capture system is used to obtain human-friendly arm motions as references for the humanoid. However the captured motions may not be applied directly to the humanoid, since the differences in geometric or dynamics aspects as length, degrees of freedom, and kinematics and dynamics capabilities exist between the humanoid and the human. To overcome this difficulty a method to adapt captured motions to a humanoid is developed. The geometric difference in the arm length is resolved by scaling the arm length of the humanoid with a constant based on a length ratio. Using the scaled geometry of the humanoid the imitation of actor's arm motion is realized by solving an inverse kinematics problem that is formulated as an optimization problem. The errors between the captured trajectories of actor arms and the approximated trajectories of humanoid arms are minimized. Such dynamics capabilities of the joint motors as limits of joint position, velocity and acceleration are also imposed on the optimization problem. Two motions of one hand waving and performing a statement in sign language are imitated by a humanoid in dynamics simulation.

1 INTRODUCTION

Interactions between a human and a robot, especially a humanoid, will have been being more important for the robot to work with the human in unknown or uncertain environment. Such interactions may require more complicated and human-like motions from a humanoid such that the motions are safe and friendly to humans. The humanoid can be controlled by planning motions or may be taught by humans to perform complex motions for working with humans. For the second case the humanoid may learn certain motions directly from a human through its cameras and other devices. In other words the humanoid will be required to move more intelligently if it lives with humans daily in the future. From this reason the humanoid needs to imitate human motions.

The process of human motion imitation begins with measuring human motions as accurately as possible. The most popular way for the measurement is to use a motion capture system that can capture the motions of a human in the form of time trajectories of markers attached on the human body. These human motions have been used for animation or human motion analysis. However those captured motions may not be applicable directly to the humanoid, since the differences between the two characters, human and humanoid, in the geometric and system aspects exist. On the other hands, the lengths, masses, and movement capabilities of the humanoid are much different from those of the human such that the appropriate conversion of the captured motions to the humanoid is needed.

The imitation of a human motion by a humanoid has been studied by some researchers. (Dasgupta and Nakamura, 1999) presented an adaptation method of human motion capture data to obtain a feasible walking pattern for a humanoid. The developed method used a Fourier expansion to determine desired trajectories of the Zero Moment Point (ZMP) from human motion capture database. An optimization problem to compute the reaction forces of the foot against the ground corresponding to the desired ZMP trajectories, was formulated. Arm motions were not however dis-

Kim C., Kim D. and Oh Y. (2005).
SOLVING AN INVERSE KINEMATICS PROBLEM FOR A HUMANOID ROBOT'S IMITATION OF HUMAN MOTIONS USING OPTIMIZATION.
In *Proceedings of the Second International Conference on Informatics in Control, Automation and Robotics - Robotics and Automation*, pages 85-92
DOI: 10.5220/0001180100850092

cussed in this work.

(Nakaoka et al., 2003) explored a procedure to let a humanoid (HRP-1S) imitate a Japanese folk dance captured by a motion capture system. Symbolic representations for primitive motions that consisted of essential arms' postures and legs' steps, were presented. The time trajectories of joint positions were first generated to imitate the primitive motions. These trajectories were then modified satisfying mechanical constraints of the humanoid. Especially, for the dynamic stabilities the trajectory of waist was modified to be consistent with the desired ZMP trajectory. The imitation of the Japanese folk dance was performed in OpenHRP dynamics simulator and was realized by the real humanoid of HRP-1S as well. As the extension of this work, (Nakaoka et al., 2004) updated the forgoing developed method. The updated method focused more on leg motions using a symbolic description of leg motion primitives in the same Japanese folk dance. By solving a inverse kinematics problem for the upper body of a human the arm motions of the humanoid were determined. The joint positions obtained from that inverse kinematics problem were then modified by the velocity limits of joint motors. The leg motions were also obtained from the inverse kinematics problem and were modified according to the desired ZMP trajectories. The entire dance was performed at the half of the speed of the original captured dance to avoid falling down.

(Pollard et al., 2002) also developed a method to adapt captured human motions to a humanoid that consists of only a upper body. The captured upper body motions of an actor was optimized, minimizing the posture differences between the humanoid and the actor. The limits of joint position and velocity of the humanoid were also involved. However, in these studies the description of the conversion of the motion capture data to the humanoid was not made in that detail.

(Zhao et al., 2004) presented a kinematics mapping of captured human motion data to a humanoid introducing a similarity function. The similarity function was defined using the errors between the joint positions of an actor and those of a humanoid. The number of degrees of freedom (DOF) of the humanoid was assumed to be same as that of the human, which may not be very realistic.

In the studies mentioned so far the procedure to obtain the trajectories of joint position and velocity of a humanoid from human motion capture data has been explored insufficiently. In other words, it was not clearly described to transform motions of a human having more DOF to the humanoid having less DOF. Therefore this work will discuss more details about that conversion process.

It is one of the key tasks for a humanoid to imitate human arm motions, since such tasks are essential in providing people with human-friendly behaviors. It is also difficult to imitate the arm motions due to complexity and delicateness of the motions. In addition, incorrect imitation of arm and hand motions may lead misunderstandings to people about the original meaning. The imitation of human arm motions will be discussed as the start of human motion imitation.

As mentioned earlier it is difficult to apply captured human arm motions to a humanoid because of several differences between a human and a humanoid as followed

- arm length difference
- length rate difference of upper and lower arms
- less degrees of freedom of a humanoid than those of a human
- dynamics capability difference

To resolve the difficulty due to the differences above an efficient method using optimization for converting captured human arm motions to a humanoid will be discussed. In addition, a simple way to impose limits of joint position and velocity will be proposed. Two human arm motions will be imitated by the humanoid in dynamics simulation to evaluate the developed method.

2 GEOMETRIC SCALING OF HUMANOID ARMS

One of the difficulties of adapting human motions to a humanoid robot is to have the work space of humanoid arms be similar to that of human arms. To resolve this difficulty (Hodgins and Pollard, 1997) proposed a rule for geometric and mass scaling to adapt existing simulated behaviors of a character to new characters. In the proposed rule the geometric scaling for running motion of a human was done using a scaling factor based on the height and the leg length of a new character. For other motions a different scaling factor was selected for more reliable animation.

In this work a scaling rule similar to (Hodgins and Pollard, 1997) is used. In detail the arm length of the humanoid robot is scaled by multiplying a dimensionless constant, $\rho = (\frac{L_{human}}{L_{robot}})$ to it. L_{human} denotes the sum of the lengths of the upper and lower arm of an actor as seen in Fig.1. L_{robot} is also defined for the humanoid in the same manner. Therefore the lengths of the upper and lower arms of humanoid are scaled as ρL_{robot}^{upper} and ρL_{robot}^{lower}. The same scaling rule is applied to the left or right arm using different scaling constants, respectively. The boundary of the work space of the arms may then become similar to the actor's. However, the scaled work space may not be identical to that of the actor due to the differences

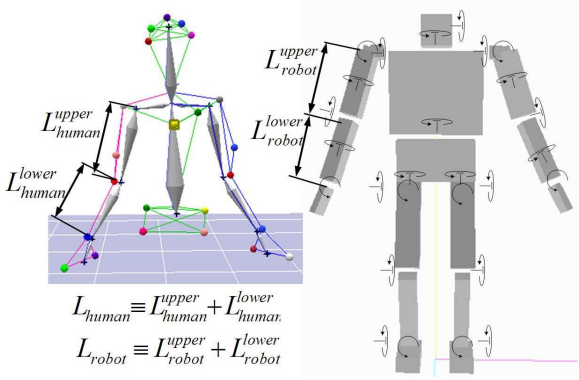

Figure 1: The upper body of a human in capturing (left) and a humanoid having 27 degrees of freedom (right).

in the length ratios of the arms. Due to this when the position and orientation of humanoid hands are imitated, the orientation of the upper arm is also forced to match with human's at the same time. Based on the scaled geometry of the humanoid the actor's arm motions are imitated by solving an inverse kinematics problem in the following section.

3 OPTIMIZATION FORMULATION FOR INVERSE KINEMATICS

Human motions can be recorded and stored using a motion capture system. It can be formulated as an inverse kinematics problem for a humanoid to perform these captured motions. In the following subsections it will be shown that this inverse kinematics problem can be formulated as an optimization problem considering motor capabilities.

3.1 Minimization of Errors in Arm and Hand Postures

The trajectories of humanoid arms can be determined using the captured position and orientation trajectories of actor's hands and upper arms as some researchers like (Lenarcic and Ravani, 1994) had done. The method presented in (Lenarcic and Ravani, 1994) is possible to solve the inverse kinematics problem discussed herein, since the humanoid has 6DOF for an arm and a hand. The method can solve the inverse kinematics problem using a generalized inverse matrix of the Jacobian of an end-effector (hand of the humanoid) and joint velocity limits. It may however be difficult to impose such more general constraints as dynamic stabilities and avoiding self-collision on those methods. Furthermore, although the position and orientation of the humanoid is successfully imitated, the arm motion of the humanoid may be matched incorrectly with that of the actor due to the difference in degrees of freedom. In other words, more accurate imitation of the hand motions may cause more errors in the motion of the upper arm, since the humanoid has less degrees of freedom, especially at the wrist, than the actor. Due to this reason a more general method is needed to minimize the errors in the trajectories of hand and upper arm simultaneously. This can be accomplished using optimization with weights on hand and upper arm motions separately. Additionally, use of optimization allows to impose more general constraints as motor capacities.

An optimization problem is formulated now to determine the optimal postures of the humanoid arms imitating the actor's arm motions captured by the motion capture system. The same optimization problem is solved repeatedly at each of the time grid points in the entire motion interval. Once the optimal posture is obtained at a certain time grid point, this posture is used as the initial value for the optimization problem for the next time grid point. Therefore, the increment of configuration of the humanoid is defined as the optimization variable as follows

$$\Delta q_{j_i} = q_{j_i} - q_{j_{i-1}} \text{ for } j = 1 \sim 6 \qquad (1)$$

where q_{j_i} is the j^{th} joint in the arm at the i^{th} time grid point. Notice that the joint numbers $j = 1 \sim 6$ are given from the shoulder to the hand for the both arms as seen in Fig.1. It is also noticed that the optimization formulation defined here can be applied to the both arms. Therefore the solution procedure will be explored for the right arm through the entire paper but it can be simply repeated to the left one as well.

Six markers were used when the motion of each arm of the actor was captured; three markers were attached on the hand (wrist, thumb, pinky), one marker at the elbow, one on the bicep, and the last one on the shoulder. First, the error between the actor hand and the humanoid hand is considered. That error is defined in terms of the distances between the three markers on the actor hand and the corresponding three points on the humanoid hand approximated from the given configuration. Secondly, the orientation error between the upper arms of the actor and the humanoid is involved. Therefore, at the i^{th} time grid point, $t = t_i$, the error function to be minimized is given as

$$\min_{\Delta\boldsymbol{\theta}_i} \; f(\Delta\boldsymbol{\theta}_i) = \mathbf{E}_{hand}(\Delta\boldsymbol{\theta}_i)^T \, W \, \mathbf{E}_{hand}(\Delta\boldsymbol{\theta}_i) + W_{10} \|\mathbf{s}_{elbow}(\Delta\boldsymbol{\theta}_i)\|^2 \qquad (2)$$

where

$$\mathbf{E}_{hand}(\Delta\boldsymbol{\theta}_i) = \begin{bmatrix} \mathbf{r}^{ac}_{wrist}(t_i) - \mathbf{r}^{hr}_{wrist}(\Delta\boldsymbol{\theta}_i) \\ \mathbf{r}^{ac}_{thumb}(t_i) - \mathbf{r}^{hr}_{thumb}(\Delta\boldsymbol{\theta}_i) \\ \mathbf{r}^{ac}_{pinky}(t_i) - \mathbf{r}^{hr}_{pinky}(\Delta\boldsymbol{\theta}_i) \end{bmatrix}$$
$$W = diag[\, W_1\, W_2\, \ldots\, W_9\,]$$
$$\Delta\boldsymbol{\theta}_i = [\, \Delta q_{1_i}\, \ldots\, \Delta q_{6_i}\,]^T \tag{3}$$

and W_{10} is a weight for the second term in Eq. (2). $\mathbf{r}^{ac}_{wrist}(t_i)$, $\mathbf{r}^{ac}_{thumb}(t_i)$ and $\mathbf{r}^{ac}_{pinky}(t_i)$ are the captured trajectories of the position vectors of three markers on the wrist, thumb and pinky of the actor hand, respectively. Similarly, three points, $\mathbf{r}^{hr}_{wrist}(\Delta\boldsymbol{\theta}_i)$, $\mathbf{r}^{hr}_{thumb}(\Delta\boldsymbol{\theta}_i)$, and $\mathbf{r}^{hr}_{pinky}(\Delta\boldsymbol{\theta}_i)$ are defined on the humanoid hand in terms of the increments of joint positions and correspond to the three points on the actor hand.

$\|\mathbf{s}_{elbow}\|$ in (2) denotes the magnitude of the vector representing the orientation difference between the upper arm of the actor and that of the humanoid as seen in Fig.2. Its square is written in terms of $\Delta\boldsymbol{\theta}_i$ as

$$\|\mathbf{s}_{elbow}(\Delta\boldsymbol{\theta}_i)\|^2 = \left\{ \frac{\mathbf{r}^{ac}_{el/sh}(t_i)^T}{\|\mathbf{r}^{ac}_{el/sh}(t_i)\|}\, \mathbf{r}^{hr}_{el/sh}(\Delta\boldsymbol{\theta}_i) \right\}^2 - \mathbf{r}^{hr}_{el/sh}(\Delta\boldsymbol{\theta}_i)^T \mathbf{r}^{hr}_{el/sh}(\Delta\boldsymbol{\theta}_i) \tag{4}$$

where

$$\mathbf{r}^{ac}_{el/sh}(t_i) = \mathbf{r}^{ac}_{el}(t_i) - \mathbf{r}^{ac}_{sh}(t_i) \tag{5}$$
$$\mathbf{r}^{hr}_{el/sh}(\Delta\boldsymbol{\theta}_i) = \mathbf{r}^{hr}_{el}(\Delta\boldsymbol{\theta}_i) - \mathbf{r}^{hr}_{sh}(\Delta\boldsymbol{\theta}_i) \tag{6}$$

where $\mathbf{r}^{ac}_{el}(t_i)$ and $\mathbf{r}^{ac}_{sh}(t_i)$ are the position vectors of the elbow and the shoulder of the actor at the time grid point, t_i, which are determined from the capture marker data. $\mathbf{r}^{hr}_{el}(\Delta\boldsymbol{\theta}_i)$ and $\mathbf{r}^{hr}_{sh}(\Delta\boldsymbol{\theta}_i)$ are the approximated position vectors of the elbow and the shoulder of the humanoid in the configuration, $\Delta\boldsymbol{\theta}_i$, at the time grid point, t_i.

As seen in Fig.2 the position and orientation of the humanoid hand are matched with those of the actor hand by minimizing the first term in the objective function in (2), since a plane can be defined by three points. This method has advantages of reducing computation efforts, since it does not need to compute the orientation angles of the hand from its rotational matrix.

Minimizing the error in the position and orientation for the hand may not be enough to imitate the entire arm motions of the actor, since the humanoid has less degrees of freedom for the arm than the actor does. Due to this the orientation error between the upper arm of the humanoid and the actor is reduced

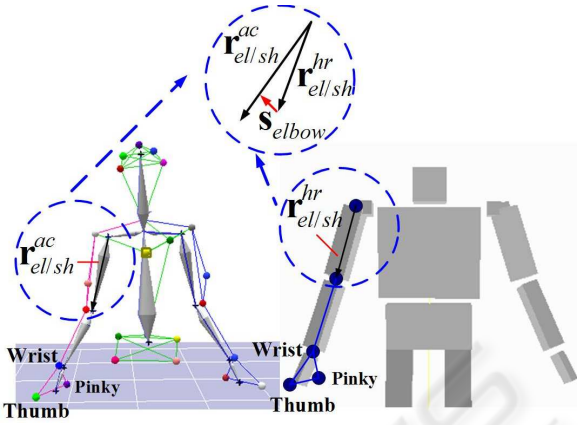

Figure 2: Marker positions on the hands of actor and humanoid, and the vector $\mathbf{s}_{elbow}$.

by minimizing the second term in Eq.(2). Therefore the proposed method does not calculate the Euler angles for the configuration from the rotational matrices given in the captured motions. This advantage allows to obtain analytical gradients of the objective function and reduce computations for the iterative optimization process.

3.2 Kinematic Constraints of Motor Capabilities

The imitation of the arm motions can be limited by several kinematic constraints as motor capabilities. The motor capabilities consist of the angle limit, velocity, and acceleration. The angle limits of the joints are imposed with easy as

$$q_j^{lower} \le q_{j_i} \le q_j^{upper} \quad \text{for } j = 1 \sim 6 \tag{7}$$

where q_j^{lower} and q_j^{upper} for $j = 1 \sim 6$ are the position limits of the joints for the arm, and $q_{j_i} = q_j(t_i)$ as in (1).

Recalling Eq.(1), the joint positions at the time, t_i, can be given in a discrete form as

$$q_{j_i} = q_{j_{i-1}} + \Delta q_{j_i} \quad \text{for } j = 1 \sim 6 \tag{8}$$

where the joint positions, $q_{j_{i-1}}$ for $j = 1 \sim 6$ are known from the previous time grid point, t_{i-1}. The inequalities in Eq.(7) are then rewritten in terms of the incremental limits of the joint positions using Eq.(8) as

$$\Delta q_j^{lower} \le \Delta q_{j_i} \le \Delta q_j^{upper} \quad \text{for } j = 1 \sim 6 \tag{9}$$

where

$$\Delta q_j^{lower} = q_j^{lower} - q_{j_{i-1}}$$
$$\Delta q_j^{upper} = q_j^{upper} - q_{j_{i-1}}. \tag{10}$$

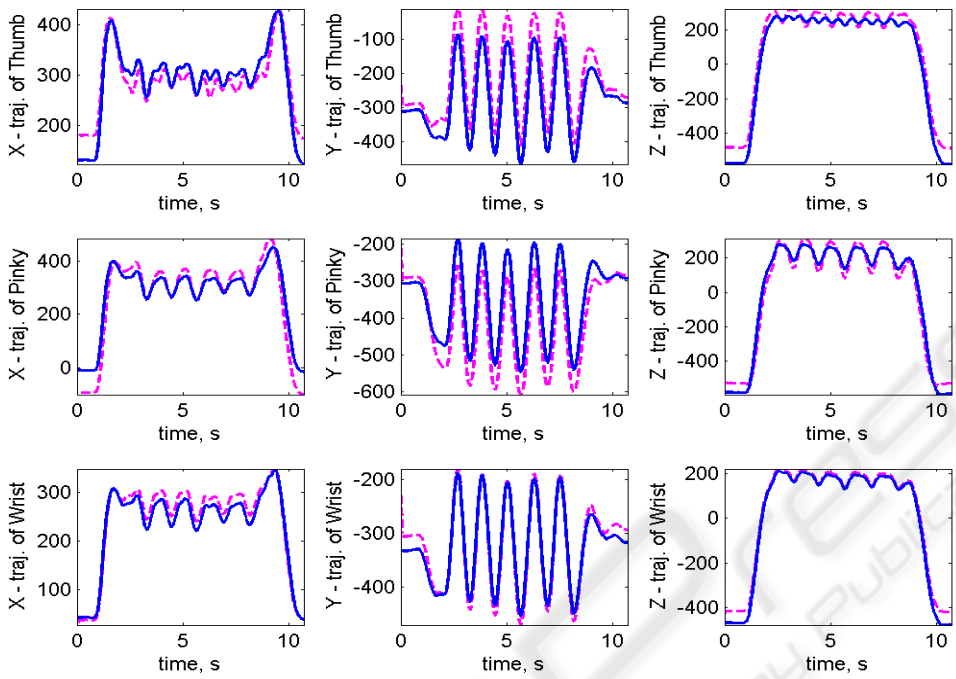

Figure 3: The marker trajectories of the actor's right hand (solid lines; mm unit) and the optimal trajectories of corresponding points on the humanoid hand (dash lines) for the motion of waving the right hand.

The capacities of motors at the joints are also limited by the bounds of motor angular velocities and accelerations as follows

$$\dot{q}_j^{lower} \leq \dot{q}_{j_i} \leq \dot{q}_j^{upper} \quad \text{for } j = 1 \sim 6 \tag{11}$$

$$\ddot{q}_j^{lower} \leq \ddot{q}_{j_i} \leq \ddot{q}_j^{upper} \quad \text{for } j = 1 \sim 6 \tag{12}$$

where $\dot{q}_j^{lower}$, $\ddot{q}_j^{lower}$, $\dot{q}_j^{upper}$, and $\ddot{q}_j^{upper}$ for $j = 1 \sim 6$ are the lower and upper bounds of the joint velocities and accelerations, respectively. The joint velocities and accelerations at t_i can be written in a discrete form using the Backward Difference Method (BDM). Using the BDM the inequalities in Eqs.(11) and (12) can be rearranged in terms of the increments of joint position at $t = t_i$ as

$$\Delta\dot{q}_j^{lower} \leq \Delta q_{j_i} \leq \Delta\dot{q}_j^{upper} \quad \text{for } j = 1 \sim 6 \tag{13}$$

$$\Delta\ddot{q}_j^{lower} \leq \Delta q_{j_i} \leq \Delta\ddot{q}_j^{upper} \quad \text{for } j = 1 \sim 6 \tag{14}$$

where

$$\begin{aligned}
\Delta\dot{q}_j^{lower} &= \Delta t\dot{q}_j^{lower} \\
\Delta\dot{q}_j^{upper} &= \Delta t\dot{q}_j^{upper} \\
\Delta\ddot{q}_j^{lower} &= \Delta t\dot{q}_j(t_{i-1}) + \Delta t^2\ddot{q}_j^{lower} \\
\Delta\ddot{q}_j^{upper} &= \Delta t\dot{q}_j(t_{i-1}) + \Delta t^2\ddot{q}_j^{upper}.
\end{aligned} \tag{15}$$

In the equations above $\dot{q}_j(t_{i-1})$ can be determined using the BDM.

The imitation of the arm motion is done by minimizing the objective function in Eq.(2) subject to sets of bounds for the joint increments in Eqs.(9), (13) and (14). This optimization problem is solved using SQP algorithm for nonlinear programming.

3.3 Gradients

In this work a gradient-based optimization scheme is used so that the analytical gradients of the objective and constraint functions are recommended to reduce optimization iterations. All the constraints in Eqs.(9), (13) and (14) are the bounds on the optimization variables, Δq_{j_i} for $j = 1 \sim 6$ such that their gradients are simply obtained. The gradient of the objective function in (2) is given as

$$\frac{\partial f}{\partial \Delta\boldsymbol{\theta}_i} = 2\Big(\frac{\partial \mathbf{E}_{hand}}{\partial \Delta\boldsymbol{\theta}_i}\Big)^T \mathbf{W}\,\mathbf{E}_{hand} + W_{10}\frac{\partial(\|\mathbf{s}_{elbow}\|^2)}{\partial \Delta\boldsymbol{\theta}_i} \tag{16}$$

where using Eqs.(3) and (4)

$$\frac{\partial \mathbf{E}_{hand}}{\partial \Delta \boldsymbol{\theta}_i} = \begin{bmatrix} -\frac{\partial \mathbf{r}^{hr}_{wrist}}{\partial \Delta \boldsymbol{\theta}_i} \\ -\frac{\partial \mathbf{r}^{hr}_{thumb}}{\partial \Delta \boldsymbol{\theta}_i} \\ -\frac{\partial \mathbf{r}^{hr}_{pinky}}{\partial \Delta \boldsymbol{\theta}_i} \end{bmatrix} = \begin{bmatrix} -\frac{\partial \mathbf{r}^{hr}_{wrist}}{\partial \boldsymbol{\theta}_i} \\ -\frac{\partial \mathbf{r}^{hr}_{thumb}}{\partial \boldsymbol{\theta}_i} \\ -\frac{\partial \mathbf{r}^{hr}_{pinky}}{\partial \boldsymbol{\theta}_i} \end{bmatrix}. \tag{17}$$

Equations (1) and (3) were used herein, since $\Delta\boldsymbol{\theta}_i = \boldsymbol{\theta}_i - \boldsymbol{\theta}_{i-1}$ and $\boldsymbol{\theta}_{i-1}$ is known. In addition,

$$\begin{aligned} \frac{\partial(\|\mathbf{s}_{elbow}\|^2)}{\partial \Delta \boldsymbol{\theta}_i} &= -\left(\frac{\partial \mathbf{r}^{hr}_{el/sh}}{\partial \Delta \boldsymbol{\theta}_i}\right)^T \mathbf{r}^{hr}_{el/sh} \\ &+ 2\left\{\frac{\mathbf{r}^{ac}_{el/sh}{}^T}{\|\mathbf{r}^{ac}_{el/sh}\|^2}\, \mathbf{r}^{hr}_{el/sh}\right\}\left(\frac{\partial \mathbf{r}^{hr}_{el/sh}}{\partial \Delta \boldsymbol{\theta}_i}\right)^T \mathbf{r}^{ac}_{el/sh} \end{aligned} \tag{18}$$

Equations (17) and (18) are determined easily, since the Jacobians of the position vectors for those equations are given analytically.

As mentioned before, since all the error terms are written in terms of the position vectors that are represented with the joint positions, the gradients above are obtained analytically. Due to the same reason computation efforts may be reduced compared with obtaining gradients numerically. The proposed method can also deal with general constraints given in terms of the position vectors such as self-collision avoidance.

4 EXAMPLES: WAVING AND SIGN LANGUAGE

To evaluate the developed method a couple of motions of an actor were captured by the Hawk Digital System commercially available from Motion Analysis Inc.. 25 markers were attached on the upper body. The motions of waving and performing a statement in sign language were recorded at the rate of 60 Hz with 642 frames and 1978 frames, respectively.

For the motion of waving the captured trajectories of the three markers on the right hand of actor and those of the corresponding three points on the right hand of humanoid are plotted in Fig.3 showing good agreements with each other. In some parts of the motion for the thumb and pinky small errors between the humanoid and the actor was observed. That may be due to the limits of joint positions and velocities of the humanoid. Therefore another procedure to compensate the motion imitated insufficiently may be needed. This is also another task for the future work. The optimal joint positions obtained from the optimization problem are shown in Fig.4. The figure also shows that the joint positions are bounded by the time varying limits obtained from the position and velocity bounds of joint motors. These varying limits are obtained from the set of bounds for the joint increments in Eqs.(9) and (13) in Sec. 3.2. It is noticed that the bounds by the acceleration limits in (14) are not considered in this work but it will have to be added in the future work. The dynamics simulation for this motion is given in Fig.5.

In Fig.6 a statement in sign language is imitated by the humanoid. The statement means, "I'd like to give hope and pleasure to you, and I love all of you.". The motion imitated is well matched with one performed by the actor.

Once the joint positions are obtained from the captured trajectories of the actor arms, the joint velocities are determined numerically. These joint positions and velocities are then applied to the humanoid as desired trajectories for controlling the humanoid with PID controller. The converted two motions are simulated in the dynamics simulator developed by the Korea Institute of Science and Technology as seen in Figs.5 and 6 .

5 DISCUSSION

A method has been proposed to transform the motion capture data of human arms to joint positions and velocities available to a humanoid. The method was able to overcome less degrees of freedom in the humanoid. The proposed method employed a general optimization scheme imposing limits on the capacities of the joint motors such that it could provide a solution procedure for an inverse kinematics problem. Since the error terms in the objective function were written in terms of only the marker's trajectories, less computation efforts were needed than obtaining Euler angles of the arms from rotational matrices. Due to this it may be useful to control a humanoid in real time. In addition it is easy to impose general constraints as the Zero Moment Point (ZMP) and self-collision avoidance on the humanoid motions, because a general optimization scheme was used. Two captured motions of waving and performing a statement in sign language have been imitated by the humanoid, showing good agreements with the captured motions through dynamics simulation. The method will be extended to whole body imitation considering dynamic balancing and self-collision avoidance in the near future.

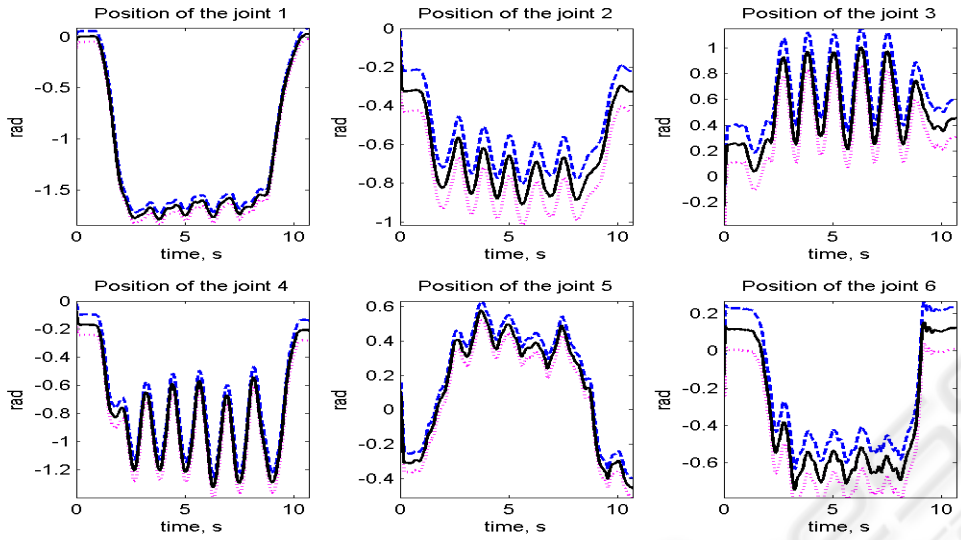

Figure 4: The optimal joint positions (solid lines) of the right arm for the motion of waving the right hand with upper (dash lines) and lower (dot lines) limits: The joints 1, 2, and 3 are for the shoulder, the joint 4 for the elbow, and the joints 5 and 6 for the wrist and the hand, respectively.

REFERENCES

Dasgupta, A. and Nakamura, Y. (1999). Making feasible walking of humanoid robots from human motion capture data. In *International Conference on Robotics and Automation*, pages 1044–1049. Detroit, Michigan.

Hodgins, J. K. and Pollard, N. S. (1997). Adapting simulated behaviors for new charaters. In *SIGGRAPH97 Proceedings*. Los Angeles, CA.

Lenarcic, J. and Ravani, B. (1994). *Advances In Robot Kinematics And Computational Geometry*. Kluwer Academic Publishers, 101 Philip Drive, Norwell, MA 02061, U.S.A., 1st edition.

Nakaoka, S., Nakazawa, A., Yokoi, K., Hirukawa, H., and Ikeuchi, K. (2003). Generating whole body motions for a biped humanoid robot from captured human dances. In *International Conference on Robotics and Automation*, pages 3905–3910. Tapei, Taiwan.

Nakaoka, S., Nakazawa, A., Yokoi, K., and Ikeuchi, K. (2004). Leg motion primitives for a dancing humanoid robot. In *International Conference on Robotics and Automation*, pages 610–615. New Orieans, LA, U.S.A.

Pollard, N. S., Hodgins, J. K., Riley, M. J., and Atkeson, C. G. (2002). Adapting human motion for the control of a humanoid robot. In *International Conference on Robotics and Automation*. Washington, DC, U.S.A.

Zhao, X., Huang, Q., Peng, Z., and Li, K. (2004). Kinematics mapping and similarity evaluation of humanoid motion based on human motion capture. In *International Conference on Intelligent RObots and Systems*. Sendai, Japan.

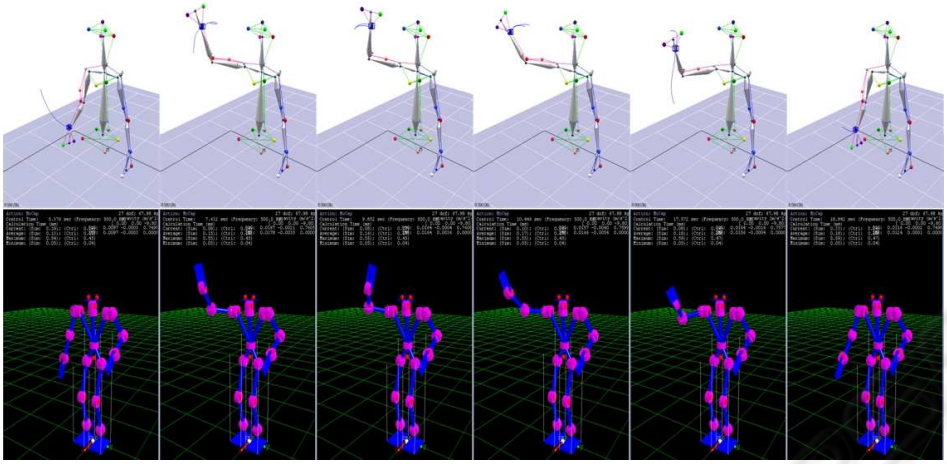

Figure 5: Waving the right hand: the captured motion of the actor (the 1^{st} row) and the motion imitated by the humanoid (the 2^{nd} row).

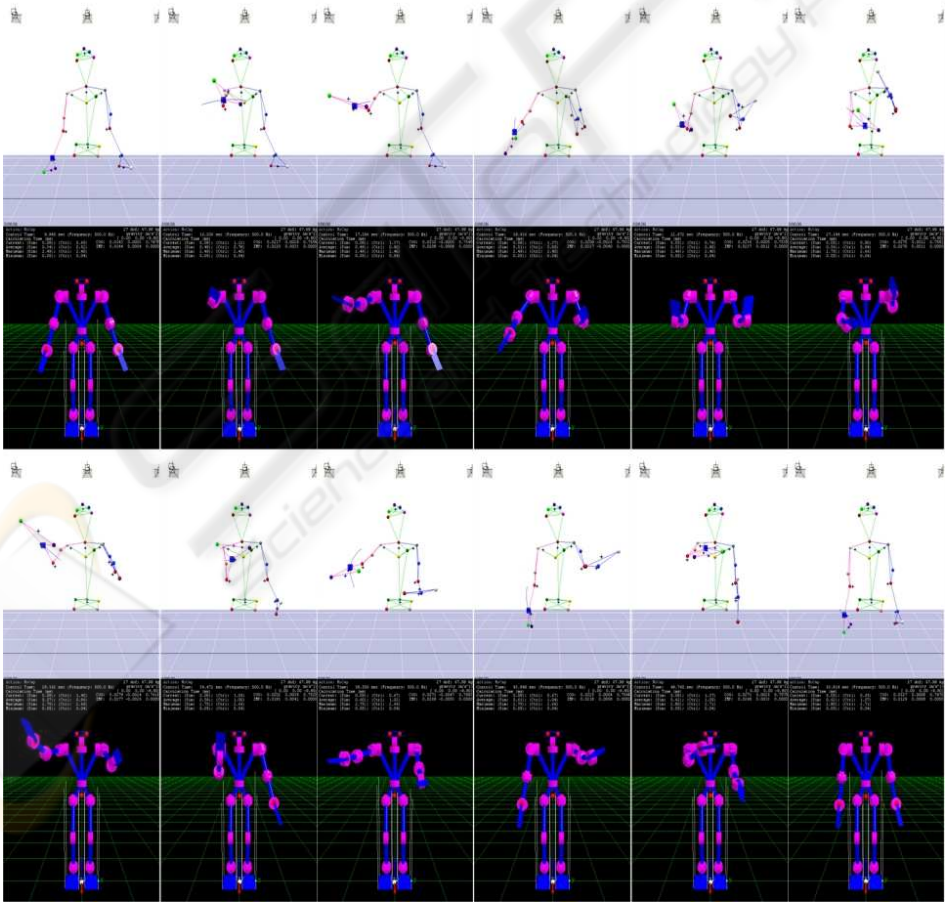

Figure 6: Sign language motions: the captured motions of the actor (the 1^{st} and 3^{rd} row) and the motions imitated by the humanoid (the 2^{nd} and 4^{th} row).